# Hippocampal Short- and Long-Term Plasticity Are Not Modulated by Astrocyte Ca 2+ Signaling

Cendra Agulhon, *et al.*

*Science* **327**, 1250 (2010);
DOI: 10.1126/science.1184821

21. Materials and methods are available as supporting material on *Science* Online.
22. N. Shakhova, I. Semiletov, G. Panteleev, *Geophys. Res. Lett.* **32**, L09601 (2005).
23. N. Shakhova, I. Semiletov, *J. Mar. Syst.* **66**, 227 (2007).
24. All the seawater-dissolved $CH_4$ concentration data are publicly and freely available at http://research.iarc.uaf.edu/SSSS/. A description of this large database as compared with previous ocean $CH_4$ studies is presented in table S3.
25. W. S. Reeburgh, *Chem. Rev.* **107**, 486 (2007).
26. I. Leifer, B. Luyendyk, J. Boles, J. Clark, *Global Biogeochem. Cycles* **20**, GB3008 (2006).
27. N. J. P. Owens, C. S. Law, R. F. C. Mantoura, P. H. Burkill, C. A. Llewellyn, *Nature* **354**, 293 (1991).
28. D. M. Karl *et al.*, *Nat. Geosci.* **1**, 473 (2008).
29. G. K. Westbrook *et al.*, *Geophys. Res. Lett.* **36**, L15608 (2009).
30. LSMM closest to the study area is established for the Barrow, Alaska, USA, monitoring station at 71° 19′ N, 156° 35′ W (www.cmdl.noaa.gov/ccgg/insitu.html); it is equal to 1.85 ppmv.
31. The division into two subpopulations for background and hotspot areas within the ESAS was based on a statistical approach detailed in SOM text S2.1 and displayed graphically in fig. S4. These two resolved populations were then first subjected to an empirical distribution function (EDF) test (SOM text S1.1). The results of the EDF test (table S1) yielded that a lognormal distribution function best fit the data. This function was hence used when applying the maximum likelihood (ML) method to calculate the statistical population parameters mean and variance [expressed as upper and lower 95% confidence limits (equations are provided in SOM text S1.1)]. The derived population parameters, displayed in table S2, were then used to estimate the overall ESAS $CH_4$ fluxes as summarized in Table 1.
32. R. Wanninkhof, *J. Geophys. Res.* **97** (C5), 7373 (1992).
33. D. D. Baldocchi, *Glob. Change Biol.* **9**, 479 (2003).
34. J. B. Edson, A. A. Hinton, K. E. Prada, J. E. Hare, C. W. Fairall, *J. Atmos. Ocean. Technol.* **15**, 547 (1998).
35. T. Fujitani, *Pap. Meteorol. Geophys.* **36**, 157 (1985).
36. We thank V. Sergienko, G. Golitsyn, S. Akasofu, L. Hinzman, and V. Akulichev for their support of our work in the Siberian Arctic. This research was supported by the International Arctic Research Centre through a National Oceanic and Atmospheric Administration Cooperative Agreement, the Far Eastern Branch of the Russian Academy of Sciences, the Russian Foundation for Basic Research, NSF, the Swedish Research Council, and the Knut and Alice Wallenberg Foundation.

**Supporting Online Material**

www.sciencemag.org/cgi/content/full/327/5970/1246/DC1
Materials and Methods
SOM Text
Figs. S1 to S4
Tables S1 to S3
References

21 September 2009; accepted 21 January 2010
10.1126/science.1182221

# Hippocampal Short- and Long-Term Plasticity Are Not Modulated by Astrocyte $Ca^{2+}$ Signaling

**Cendra Agulhon,[1]* Todd A. Fiacco,[2] Ken D. McCarthy[1]**

The concept that astrocytes release neuroactive molecules (gliotransmitters) to affect synaptic transmission has been a paradigm shift in neuroscience research over the past decade. This concept suggests that astrocytes, together with pre- and postsynaptic neuronal elements, make up a functional synapse. Astrocyte release of gliotransmitters (for example, glutamate and adenosine triphosphate) is generally accepted to be a $Ca^{2+}$-dependent process. We used two mouse lines to either selectively increase or obliterate astrocytic $G_q$ G protein–coupled receptor $Ca^{2+}$ signaling to further test the hypothesis that astrocytes release gliotransmitters in a $Ca^{2+}$-dependent manner to affect synaptic transmission. Neither increasing nor obliterating astrocytic $Ca^{2+}$ fluxes affects spontaneous and evoked excitatory synaptic transmission or synaptic plasticity. Our findings suggest that, at least in the hippocampus, the mechanisms of gliotransmission need to be reconsidered.

Calcium transients in astrocytes are physiologically driven by metabotropic $G_q$ G protein–coupled receptors ($G_q$ GPCRs), which can be activated after neurotransmitter release from presynaptic terminals (*1*, *2*). At Schaffer collateral-CA1 (SC-CA1) synapses in acute hippocampal slices, astrocytes can modulate neuronal activity by elevations in $Ca^{2+}$ that are evoked by the following: (i) uncaging $IP_3$ or $Ca^{2+}$ in individual astrocytes, (ii) repetitive depolarization of the astrocyte membrane, (iii) mechanical stimulation of an astrocyte, or (iv) bath application of endogenous $G_q$ GPCR agonists. With these pharmacological approaches, astrocyte $Ca^{2+}$ elevations have been reported to trigger gliotransmitter release from astrocytes, resulting in the modulation of synaptic transmission and plasticity through the activation of presynaptic [for example, group I metabotropic glutamate receptors (mGluRs) or adenosine A(1) receptors ($A_1$Rs)] or postsynaptic receptors [*N*-methyl-D-aspartate receptors (NMDARs)] (*3*–*11*). To circumvent a number of caveats associated with the pharmacological approaches described above (*12*–*15*), we have recently developed and characterized two genetically modified mice [the MrgA1$^+$ and $IP_3$R2 knockout (KO) mice] that enable either selective activation or inactivation of $G_q$ GPCR $Ca^{2+}$ signaling in astrocytes (*13*, *16*, *17*). Within the hippocampus, the stimulation of transgenic MrgA1 $G_q$ GPCRs leads to astrocyte-specific $Ca^{2+}$ responses that mimic the "$Ca^{2+}$ fingerprint" response that is elicited by endogenous $G_q$ GPCRs (*13*). In hippocampal slices derived from $IP_3$R2 KO mice (*17*), $G_q$ GPCR $Ca^{2+}$ signaling is obliterated selectively in 100% of astrocytes without affecting neuronal $Ca^{2+}$ responses (*16*).

We first tested the possibility that astrocytic $G_q$ GPCR $Ca^{2+}$ is involved in the modulation of spontaneous excitatory postsynaptic currents (sEPSCs). In these and the following experiments, a high percentage of astrocytes (~90 to 100%) were stimulated so that each CA1 neuron has the vast majority of its synapses embedded in astrocyte processes that elevate $Ca^{2+}$ upon $G_q$ GPCR agonist application. Control experiments showed that MrgA1R expression by itself in astrocytes does not affect basal neuronal activity in a nonspecific manner [supporting online material (SOM) text S1]. MrgA1R agonist Phe-Met-Arg-Phe-$NH_2$ amide (FMRF, 15 μM) was applied to trigger $Ca^{2+}$ elevations in ~90% of mature MrgA1$^+$ passive astrocytes (*13*) in cell bodies as well as fine processes (Fig. 1, A and B, boxes/traces 1 to 5, SOM text S2, and movie S1). No significant effect of astrocyte $Ca^{2+}$ elevations on sEPSC frequency and amplitude in CA1 neurons from MrgA1$^+$ mice was found (Fig. 1C and SOM text S3, $n = 7$, $P > 0.05$). To test the possibility that this lack of effect might be caused by the stimulation of a transgenic $G_q$ GPCR, we also stimulated endogenous astrocytic endothelin $G_q$ GPCRs (ETRs), which were selected as optimal candidates because they evoke gliotransmitter release in vitro (*18*), they are thought to be very weakly expressed by neurons and heavily expressed by brain astrocytes at postnatal day 1 to 30 (*19*), and no direct effects on neuronal activity have been reported when stimulating ETRs (*13*). Astrocytic ETR-mediated $Ca^{2+}$ increases in ~100% of astrocytes from wild-type (WT) hippocampal slices [endothelin 1 (ET1) and ET3, 10 nM each; SOM text S4, and fig. S1) had no effect on the frequency or amplitude of sEPSCs (Fig. 1, D to F, and SOM text S5, $n = 5$, $P > 0.05$).

Previous studies using conventional pharmacological approaches have suggested that postsynaptic NMDARs might be preferential targets for glutamate release from astrocytes (*3*–*7*, *9*, *10*), prompting us to examine the possibility that astrocytic $G_q$ GPCR $Ca^{2+}$ elevations modulate the NMDAR-mediated component of evoked whole-cell EPSCs (eEPSCs). FMRF does not produce a nonspecific effect on NMDA eEPSCs (Fig. 2, A and A1, and SOM text S6). FMRF or ETs were

[1]Department of Pharmacology, University of North Carolina at Chapel Hill, Genetic Medicine Building, CB 7365, Chapel Hill, NC 27599, USA. [2]Department of Cell Biology and Neuroscience, University of California Riverside, Riverside, CA 92521, USA.

*To whom correspondence should be addressed. E-mail: cendra_agulhon@med.unc.edu

applied to MrgA1$^+$ or WT slices, respectively, and the amplitude of NMDA eEPSCs was unaffected during agonist-mediated $Ca^{2+}$ increases in astrocytes (Fig. 2, B and B1, and SOM text S7, MrgA1$^+$, $n = 11$, $P > 0.05$; Fig. 2, C and C1, and SOM text S7, WT, $n = 7$, $P > 0.05$).

Uncaging $IP_3$ or $Ca^{2+}$ in astrocytes produces a transient enhancement of the probability of neurotransmitter release at a fraction of the SC terminals (*10*, *20*). We directly tested whether activating or inactivating astrocytic $G_q$ GPCR $Ca^{2+}$ signaling affects presynaptic release probability and short-term plasticity by measuring the paired-pulse facilitation (PPF) index of evoked field potentials (fEPSPs). Astrocytic MrgA1R expression by itself did not have a nonspecific effect on PPF (Fig. 2D and SOM text S8). No overall PPF profile changes were observed in association with astrocyte MrgA1R- or ETR-mediated $Ca^{2+}$ elevations in MrgA1$^+$ or WT slices, respectively (Fig. 2E, MrgA1$^+$, $n = 7$, $P > 0.05$; Fig. 2F, WT, $n = 6$, $P > 0.05$). We reasoned that if astrocytic $Ca^{2+}$ elevations regulate gliotransmitter release, then the removal of astrocytic $G_q$ GPCR $Ca^{2+}$ signaling should affect tonic and activity-induced gliotransmitter release and, consequently, PPF. Therefore, PPF was measured in $IP_3R2$ KO mice versus WT littermate controls. Again, no changes in PPF profiles were observed between the two groups (Fig. 2G, $IP_3R2$ KO, $n = 9$; WT, $n = 9$; $P = 0.73$).

A recent study has shown that temporal coincidence of astrocyte $Ca^{2+}$ elevations (evoked by $Ca^{2+}$ uncaging) and transient depolarization of CA1 neurons can induce a presynaptic form of long-term potentiation (LTP) in SC-CA1 synapses (*10*). Therefore, stimulating astrocytic $G_q$ GPCR $Ca^{2+}$ signaling simultaneously with depolarization of large ensembles of CA1 neurons should either directly induce LTP or at least modulate the baseline slope of fEPSPs through gliotransmitter activation of presynaptic group I mGluRs, or, alternatively, $A_1$Rs (*10*, *21*). Our data do not support these predictions (fig. S2, B, B1, C, C1, and SOM text S9).

We also directly tested whether astrocytic $G_q$ GPCRs regulate LTP magnitude as well as post-tetanic potentiation (PTP). Similar to PPF, PTP is a form of short-term plasticity (*22*). First, a battery of control experiments clearly demonstrated that neither the selective astrocytic expression of MrgA1Rs nor the application of FMRF to WT slices affected input-output (I/O) curves, PTP, or LTP (Fig. 3, A and D, and SOM text S10). A prerequisite for the involvement of astrocytes in LTP is that their activation precedes the induction of LTP. After establishing a 15-min baseline recording of fEPSPs, $Ca^{2+}$ elevations in astrocytes were induced by bath application of either FMRF to MrgA1$^+$ slices or ETs to WT slices. LTP was induced ~2.5 min after agonist application, when the peaks of $Ca^{2+}$ responses in astrocytes reached their maximum (Fig. 3, B and C). LTP magnitudes obtained from MrgA1$^+$ slices



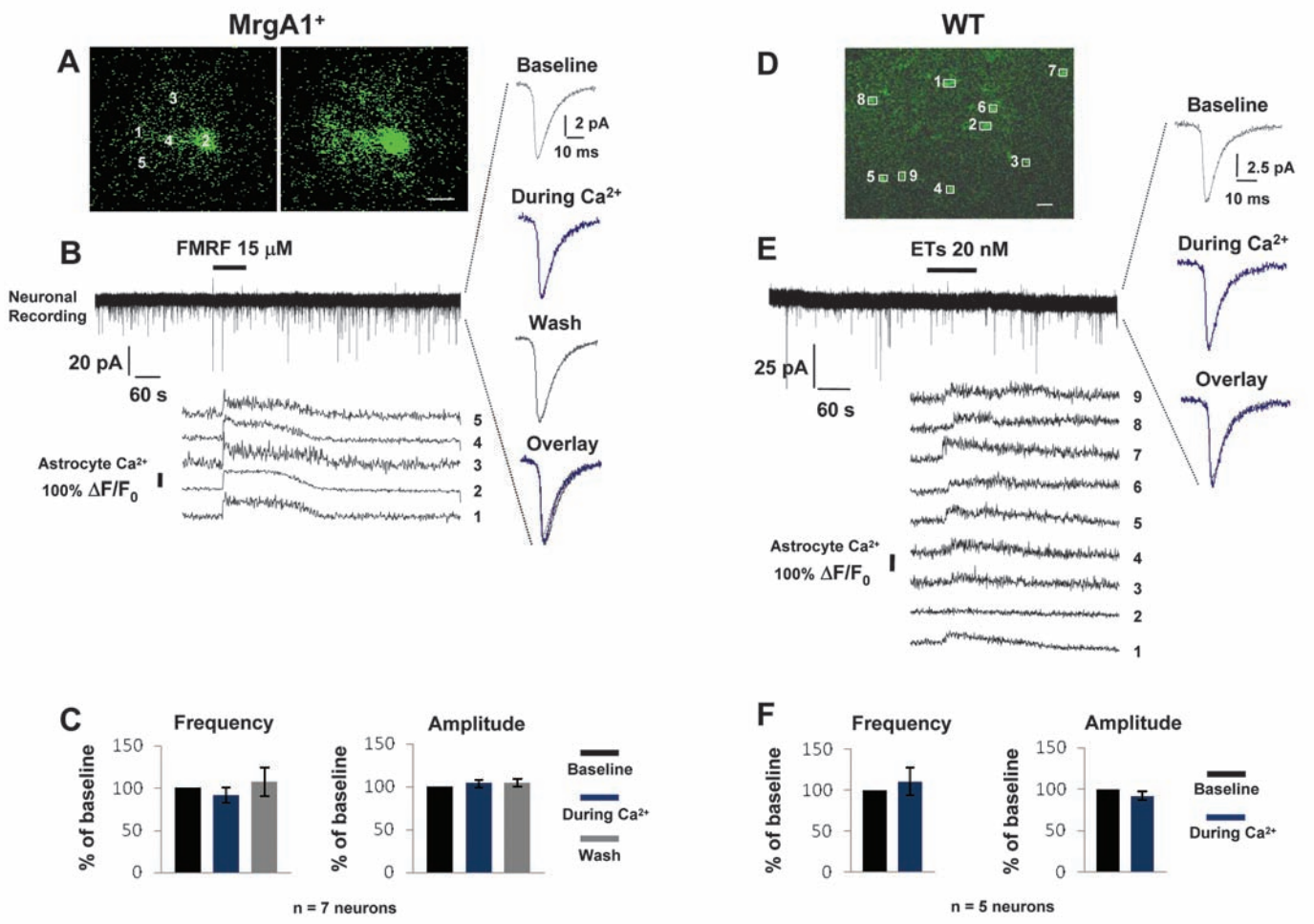


**Fig. 1.** Stimulation of astrocytic $G_q$ GPCRs does not affect sEPSCs in CA1 pyramidal neurons. (**A**) Typical MrgA1$^+$ astrocyte in stratum radiatum (s.r.), filled with Oregon-Green-BAPTA-1 (OGB1), before (left) and after (right) stimulation of MrgA1Rs with FMRF (15 μM). Astrocyte $Ca^{2+}$ responses are included as representative responses of the ~90% of responsive astrocytes within the slice and were used to monitor the beginning of $Ca^{2+}$ elevations relative to neuronal activity. (**B** and **C**) sEPSCs frequency and amplitude remain unchanged [(B), upper] during astrocyte $Ca^{2+}$ increases [(B), traces 1 to 5]. To the right are the averaged sEPSCs from the trace in (B). (**D**) Astrocytes (1 to 9) bulk-loaded with $Ca^{2+}$ green 1-AM in s.r. from WT slices. (**E** and **F**) sEPSCs frequency and amplitude were unchanged during astrocyte ETR-mediated $Ca^{2+}$ increases (ET1 and ET3, 10 nM each). Due to long-tailing ETR $Ca^{2+}$ increases, sEPSCs were analyzed only during the first 120 s of astrocyte $Ca^{2+}$ increases. Scale bars in (A) and (D) indicate 10 and 20 μm, respectively. Error bars indicate SEM.

stimulated with FMRF (137.97 ± 5.58%, $n = 14$ slices) or WT slices stimulated with ETs (133.13 ± 7.62%, $n = 9$), respectively, were no different from LTP magnitudes obtained in matching controls (Fig. 3, E and F, and SOM text S11, $P > 0.05$). Furthermore, PTP was also not affected (Fig. 3, E and F, and SOM text S11, $P > 0.05$).

Next, we examined whether the obliteration of astrocytic $G_q$ GPCR $Ca^{2+}$ signaling would affect basal synaptic transmission as well as PTP and LTP. No significant difference was found in I/O curves performed in $IP_3R2$ KO versus WT littermate control mice (Fig. 3G, $IP_3R2$ KO, $n = 21$; WT, $n = 18$; $P = 0.94$). These results indicate that both the pre- and postsynaptic responses, and thus the basal SC-evoked synaptic transmission, are intact in $IP_3R2$ KO mice, even though astrocytes are completely incapable of producing $G_q$ GPCR $Ca^{2+}$ elevations. No significant alteration in PTP and LTP was detected between $IP_3R2$ KO and control mice, demonstrating that astrocytic $G_q$ GPCR–mediated $Ca^{2+}$ signaling does not account for a tonic form nor an activity-induced form of short- and long-term synaptic plasticity (Fig. 3H and SOM text S12, $IP_3R2$ KO, $n = 10$; WT, $n = 8$, $P > 0.05$). To validate these $IP_3R2$ KO data, we showed that the LTP stimulation protocol used is sufficient to induce $Ca^{2+}$ increases in astrocytes from WT slices (fig. S3). Finally, we also found that stimulating or removing astrocytic $G_q$ GPCR $Ca^{2+}$ signaling in $MrgA1^+$ or $IP_3R2$ KO mice, respectively, does not significantly alter LTP and PTP induced by theta-burst stimulation (SOM text S13).

Previous studies have demonstrated that activation of synaptic group I mGluRs, $A_1$Rs, or NMDARs depotentiates LTP at SC-CA1 synapses (*23*–*27*). These three receptors have all been reported to be the targets of astrocytic $Ca^{2+}$-dependent sources of glutamate or adenosine triphosphate (ATP)/adenosine under certain conditions (*12*). To further test whether astrocytic $G_q$ GPCR $Ca^{2+}$ signaling is sufficient to induce gliotransmitter release to affect synaptic transmission through the activation of synaptic mGluRs, $A_1$Rs, or NMDARs, we investigated the role of astrocyte $Ca^{2+}$ signaling in the maintenance of LTP. Fifty minutes after LTP induction, astrocyte $Ca^{2+}$ increases were elicited by applications of FMRF to $MrgA1^+$ slices or of ETs to WT slices. This did not lead to a significant change in the slope of fEPSPs (Fig. 4, A, B, and D, and SOM text S14, $n = 9$ $MrgA1^+$ slices, $n = 16$ WT slices, $P > 0.05$). As a positive control for agonist-induced depotentiation, we applied (RS)-3,5-dihydroxyphenylglycine (DHPG, 50 μM), which exerted a significant depotentiation of the slope in all slices tested (Fig. 4, A and D; $MrgA1^+$, 74.82 ± 3.45%, $n = 12$, $P <$



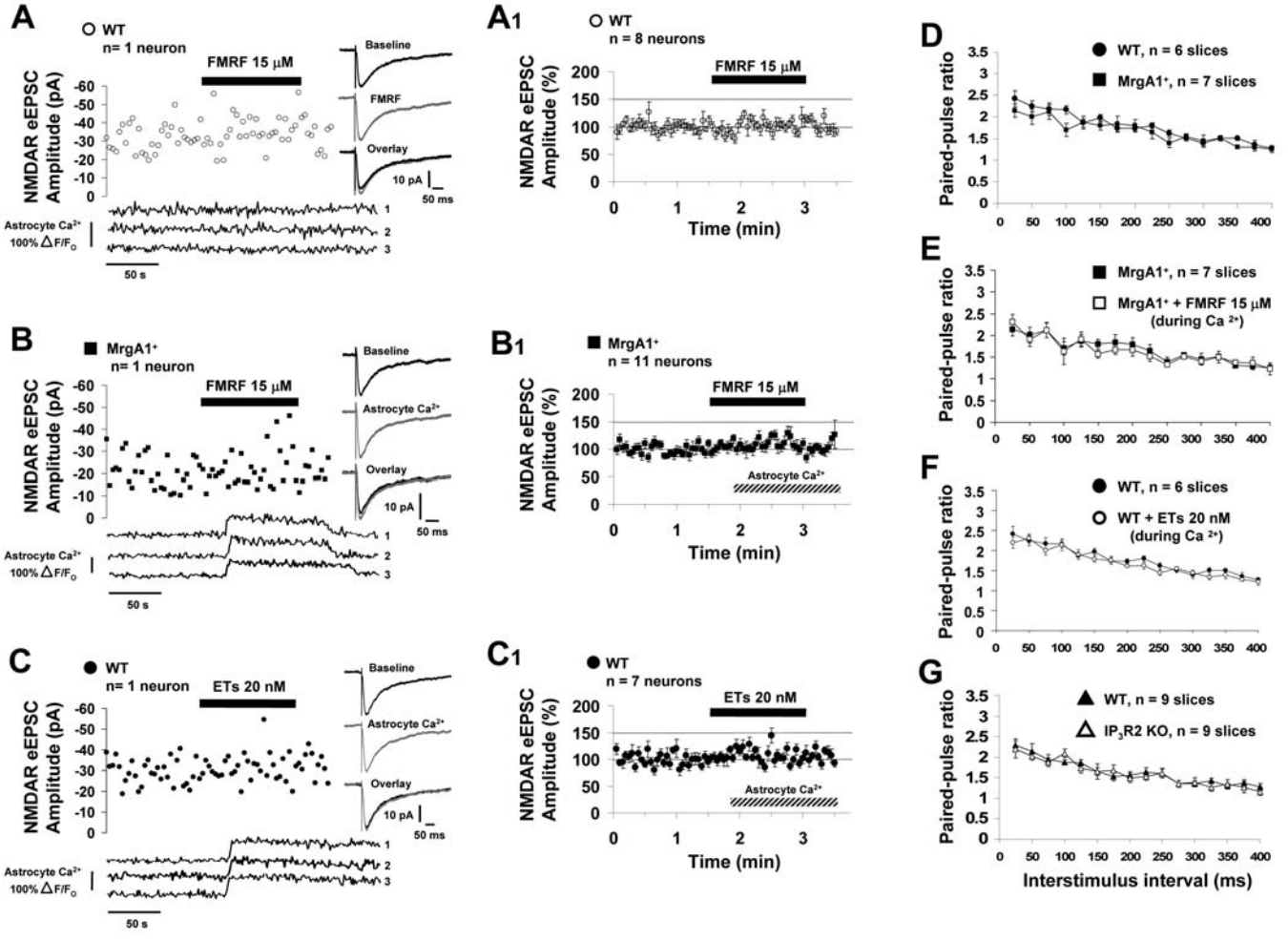


**Fig. 2.** Astrocytic $G_q$ GPCR $Ca^{2+}$ signaling does not modulate the NMDA eEPSC peak amplitude or PPF in CA1 pyramidal neurons. (**A** and **A1**) WT astrocytes were not activated by FMRF [(A) lower $Ca^{2+}$ traces from three astrocytes surrounding recorded neuron]. FMRF did not nonspecifically affect NMDA eEPSC peak amplitude in WT mice. Representative example (A) and pooled data (A1). (**B**, **B1**, **C**, and **C1**) Activation of $MrgA1^+$ (B and B1) or WT astrocytes (C and C1) by FMRF or ETs, respectively, did not affect NMDA eEPSC peak amplitude. (**D**) MrgA1R expression in astrocytes of $MrgA1^+$ mice did not have a nonspecific effect on PPF ratio compared with WT littermate mice. (**E** and **F**) PPF ratios in $MrgA1^+$ slices before (solid squares) and during (open squares) FMRF-evoked astrocyte $Ca^{2+}$ elevations (E) or in WT slices before (solid circles) and during (open circles) ET-evoked astrocyte $Ca^{2+}$ increases (F) were not significantly different. (**G**) PPF is not altered in $IP_3R2$ KO mice compared with WT littermate control mice.

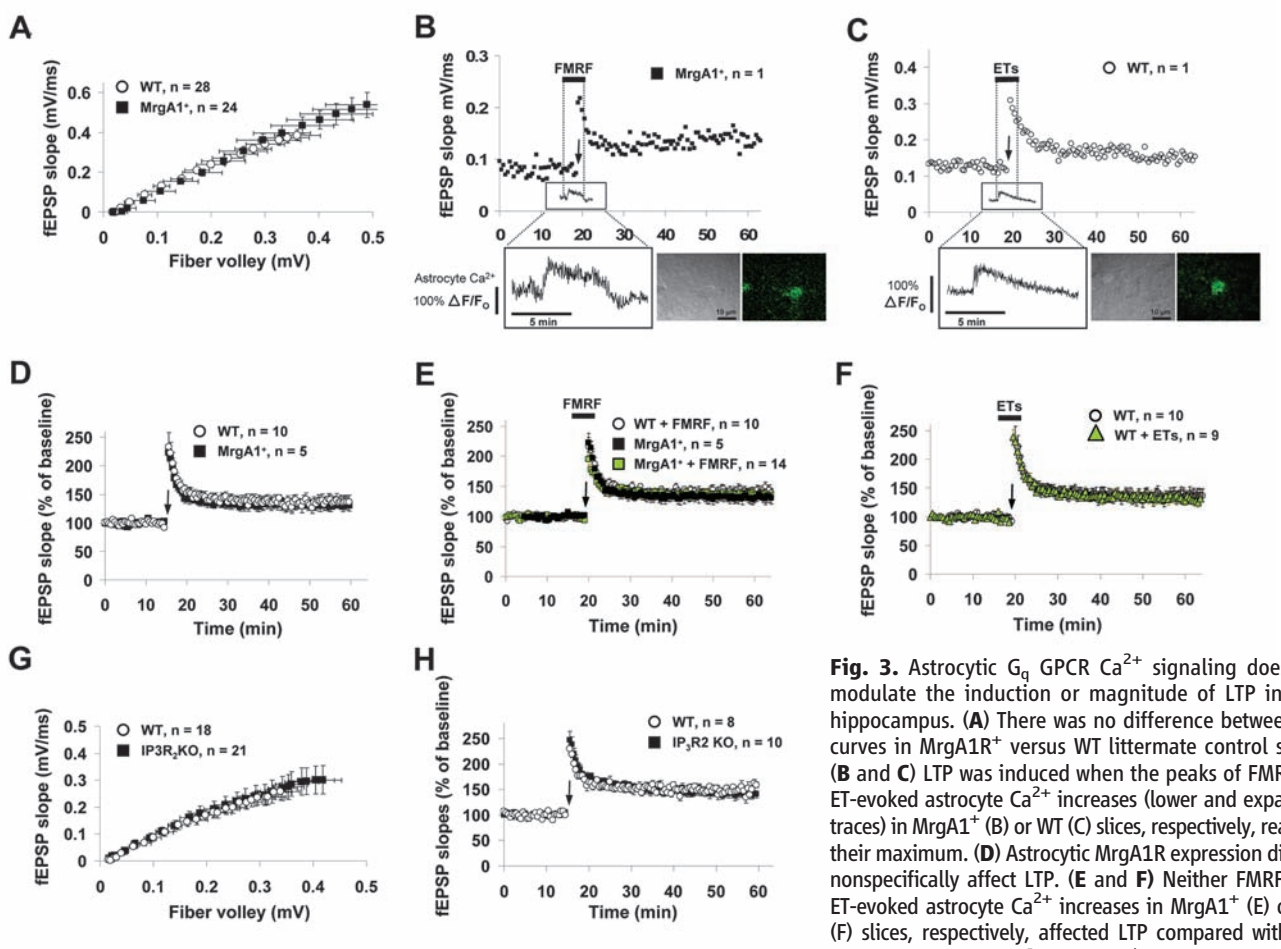


**Fig. 3.** Astrocytic $G_q$ GPCR $Ca^{2+}$ signaling does not modulate the induction or magnitude of LTP in CA1 hippocampus. (**A**) There was no difference between I/O curves in MrgA1R$^+$ versus WT littermate control slices. (**B** and **C**) LTP was induced when the peaks of FMRF- or ET-evoked astrocyte $Ca^{2+}$ increases (lower and expanded traces) in MrgA1$^+$ (B) or WT (C) slices, respectively, reached their maximum. (**D**) Astrocytic MrgA1R expression did not nonspecifically affect LTP. (**E** and **F**) Neither FMRF- nor ET-evoked astrocyte $Ca^{2+}$ increases in MrgA1$^+$ (E) or WT (F) slices, respectively, affected LTP compared with two sets of control slices [(E), MrgA1$^+$ slices without FMRF application, WT littermate slices with FMRF application; (F), WT slices without ET application]. (**G** and **H**) I/O curves (G) and LTP (H) in $IP_3R2$ KO mice are not affected compared with WT littermate control mice. Arrows indicate LTP induction (2 × 100 Hz).

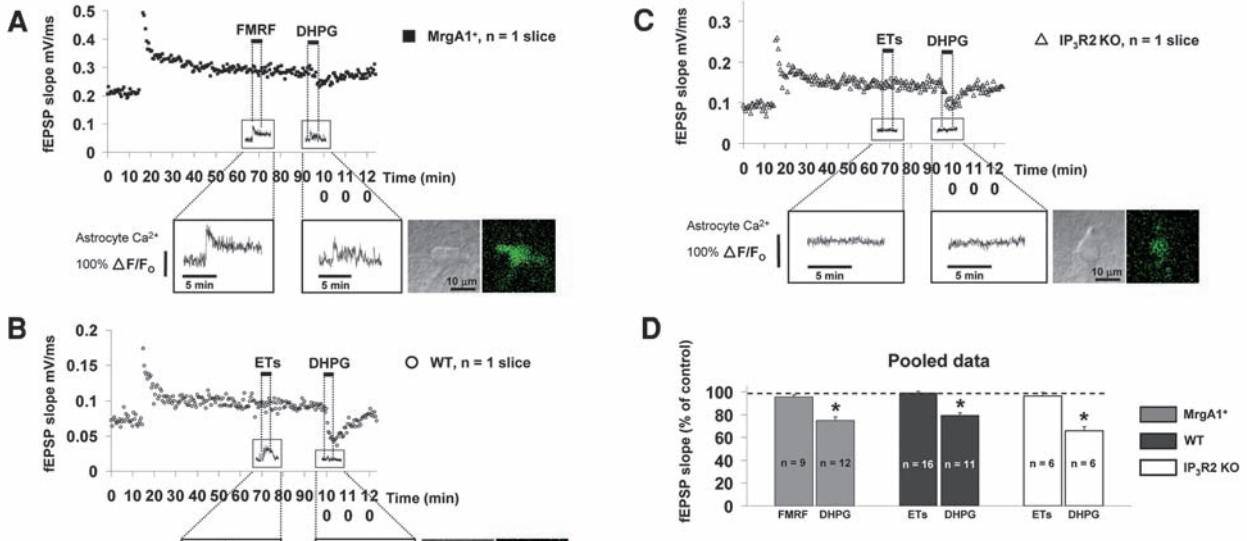


**Fig. 4.** Astrocytic $G_q$ GPCR $Ca^{2+}$ signaling does not modulate the maintenance of LTP (2 × 100 Hz) in CA1 hippocampus. (**A** and **B**) Neither FMRF- nor ET-evoked astrocyte $Ca^{2+}$ increases (lower and expanded traces) in MrgA1$^+$ slices (A) or WT slices (B), respectively, modulated the maintenance of LTP. As a control for modulation of LTP maintenance, DHPG (50 μM) was applied. (**C**) ETs and DHPG did not evoke any astrocyte $Ca^{2+}$ increases in $IP_3R2$ KO slices. Whereas ETs did not modulate the maintenance of LTP, DHPG induced a clear depotentiation independent of astrocyte $Ca^{2+}$ elevations. (**D**) Summary histogram showing that DHPG, but not FMRF or ETs, affected the maintenance of LTP in MrgA1$^+$, WT, or $IP_3R2$ KO slices. Asterisks indicate statistical significance ($P < 0.0001$).

0.0001; Fig. 4, B and D; WT, 79.54 ± 2.03%, $n$ = 11, $P < 0.0001$). To address the possibility that the DHPG-mediated depotentiation could be due in part to astrocyte $Ca^{2+}$, we performed the same experiments using $IP_3R2$ KO mice. The magnitude of DHPG-induced depotentiation in $IP_3R2$ KO slices was not only significant ($P < 0.0001$), it was also similar to the magnitude of depotentiation that was recorded in WT littermate slices ($P = 0.43$), indicating that depotentiation does not rely, even in part, on $Ca^{2+}$-dependent gliotransmitter release from astrocytes (Fig. 4, C and D; $IP_3R2$ KO, 66.95 ± 2.79%, $n$ = 6; WT, 72.70 ± 5.72%, $n$ = 8). These results demonstrate and confirm previous data that DHPG-induced modulation of neuronal activity (*28*, *29*), such as depotentiation (*26*), is due to the direct action of DHPG on neuronal group I mGluRs (*26*), and not to astrocytic group I mGluR-mediated $Ca^{2+}$ elevations and putative gliotransmitter release.

We provide here strong evidence that $G_q$ GPCR $Ca^{2+}$ signaling in astrocytes does not affect spontaneous and evoked excitatory action potential (AP)-mediated synaptic transmission or short- and long-term plasticity at the SC-CA1 synapse. We used two molecular tools (the $MrgA1^+$ and $IP_3R2$ KO mouse models), as well as the activation of endogenous astrocytic $G_q$ GPCRs, to manipulate $Ca^{2+}$ in astrocytes. A battery of eight electrophysiological protocols (sEPSCs, NMDA eEPSCs, evoked AMPA fEPSPs, I/O curves, PPF, PTP, and two forms of LTP) were studied, all of which point to a lack of modulation of excitatory AP-mediated synaptic transmission by astrocytic $G_q$ GPCR $Ca^{2+}$ signaling. The most logical conclusion from the present analysis is that astrocytic $G_q$ GPCRs and $Ca^{2+}$ signaling activity are not tied to the release of gliotransmitters affecting synaptic transmission or short and long-term plasticity. Therefore, our results suggest that gliotransmission reflects the pharmacological approaches that were used in previous studies (*3*–*10*, *12*) and, at least within the hippocampus, does not occur when the endogenous regulators of astrocyte $Ca^{2+}$, the $G_q$ GPCRs, or the $IP_3R2$ themselves are stimulated or inactivated in a cellular-selective manner. These findings suggest that the mechanisms of gliotransmitter release should be reconsidered. These results have profound implications for our understanding of synaptic transmission and should affect the interpretation of a broad range of findings. Thus, the purpose of neuron-to-astrocyte $G_q$ GPCR $Ca^{2+}$ signaling in neurophysiology remains an open question.

### References and Notes


1. X. Wang *et al.*, *Nat. Neurosci.* **9**, 816 (2006).
2. J. T. Porter, K. D. McCarthy, *J. Neurosci.* **16**, 5073 (1996).
3. M. C. Angulo, A. S. Kozlov, S. Charpak, E. Audinat, *J. Neurosci.* **24**, 6920 (2004).
4. T. Fellin *et al.*, *Neuron* **43**, 729 (2004).
5. C. J. Lee *et al.*, *J. Physiol.* **581**, 1057 (2007).
6. M. Navarrete, A. Araque, *Neuron* **57**, 883 (2008).
7. L. Pasti, A. Volterra, T. Pozzan, G. Carmignoto, *J. Neurosci.* **17**, 7817 (1997).
8. G. Perea, A. Araque, *J. Neurosci.* **25**, 2192 (2005).
9. E. Shigetomi, D. N. Bowser, M. V. Sofroniew, B. S. Khakh, *J. Neurosci.* **28**, 6659 (2008).
10. G. Perea, A. Araque, *Science* **317**, 1083 (2007).
11. A. Serrano, N. Haddjeri, J. C. Lacaille, R. Robitaille, *J. Neurosci.* **26**, 5370 (2006).
12. C. Agulhon *et al.*, *Neuron* **59**, 932 (2008).
13. T. A. Fiacco *et al.*, *Neuron* **54**, 611 (2007).
14. T. A. Fiacco, C. Agulhon, K. D. McCarthy, *Annu. Rev. Pharmacol. Toxicol.* **49**, 151 (2009).
15. N. X. Tritsch, D. E. Bergles, *Neuron* **54**, 497 (2007).
16. J. Petravicz, T. A. Fiacco, K. D. McCarthy, *J. Neurosci.* **28**, 4967 (2008).
17. X. Li, A. V. Zima, F. Sheikh, L. A. Blatter, J. Chen, *Circ. Res.* **96**, 1274 (2005).
18. Y. Sasaki *et al.*, *J. Neurochem.* **68**, 2194 (1997).
19. M. Andersson, F. Blomstrand, E. Hanse, *J. Physiol.* **585**, 843 (2007).
20. T. A. Fiacco, K. D. McCarthy, *J. Neurosci.* **24**, 722 (2004).
21. O. Pascual *et al.*, *Science* **310**, 113 (2005).
22. R. S. Zucker, *Neuron* **17**, 1049 (1996).
23. H. J. Chung *et al.*, *Proc. Natl. Acad. Sci. U.S.A.* **106**, 635 (2009).
24. C. C. Huang, Y. C. Liang, K. S. Hsu, *J. Biol. Chem.* **276**, 48108 (2001).
25. R. Li, F. S. Huang, A. K. Abbas, H. Wigström, *BMC Neurosci.* **8**, 55 (2007).
26. W. M. Zho, J. L. You, C. C. Huang, K. S. Hsu, *J. Neurosci.* **22**, 8838 (2002).
27. Y. Izumi, C. F. Zorumski, *J. Neurosci.* **28**, 9557 (2008).
28. G. Mannaioni, M. J. Marino, O. Valenti, S. F. Traynelis, P. J. Conn, *J. Neurosci.* **21**, 5925 (2001).
29. M. G. Rae, A. J. Irving, *Neuropharmacology* **46**, 1057 (2004).


30. We thank K. Casper for making $MrgA1^+$ mice; J. Chen for providing $IP_3R2$ KO mice; and B. Djukic, B. Philpot, A. Roberts, and J. de Marchena for valuable help and discussions. This work was supported by NIH grants NS033938 and NS020212.


### Supporting Online Material

www.sciencemag.org/cgi/content/full/327/5970/1250/DC1
Materials and Methods
SOM Text S1 to S14
Figs. S1 to S3
References
Movie S1

17 November 2009; accepted 19 January 2010
10.1126/science.1184821

# RTEL-1 Enforces Meiotic Crossover Interference and Homeostasis

**Jillian L. Youds,[1] David G. Mets,[2] Michael J. McIlwraith,[3] Julie S. Martin,[1] Jordan D. Ward,[1]* Nigel J. ONeil,[4] Ann M. Rose,[4] Stephen C. West,[3] Barbara J. Meyer,[2] Simon J. Boulton[1]†**

**Meiotic crossovers (COs) are tightly regulated to ensure that COs on the same chromosome are distributed far apart (crossover interference, COI) and that at least one CO is formed per homolog pair (CO homeostasis). CO formation is controlled in part during meiotic double-strand break (DSB) creation in *Caenorhabditis elegans*, but a second level of control must also exist because meiotic DSBs outnumber COs. We show that the anti-recombinase RTEL-1 is required to prevent excess meiotic COs, probably by promoting meiotic synthesis-dependent strand annealing. Two distinct classes of meiotic COs are increased in *rtel-1* mutants, and COI and homeostasis are compromised. We propose that RTEL-1 implements the second level of CO control by promoting noncrossovers.**

Homologous recombination repair of meiotic DNA double-strand breaks (DSBs) is regulated to ensure the correct number and placement of meiotic crossovers (COs). One CO per chromosome ensures that homologous chromosomes are held together, can orient toward opposite spindle poles, and thereby segregate correctly at the first meiotic division. Crossover interference (COI) ensures appropriate distribution of COs among chromosomes because the formation of one CO reduces the likelihood of other COs occurring nearby. Meiotic COI is "complete" in *Caenorhabditis elegans*: Only a single CO occurs on each chromosome (*1*, *2*). COI is regulated in part by the condensin I complex, which limits meiotic DSB formation (*3*). Because the average number of meiotic DSBs per chromosome is 2.1 (*3*), and only one of these is repaired as a CO, a second tier of CO control must exist downstream of meiotic DSB formation that channels about half of all DSBs into noncrossovers (NCOs). However, the proteins involved in generating a meiotic CO versus NCO are not well understood.

Human RTEL1 (and *C. elegans* RTEL-1, by homology) negatively regulates recombination by disassembling D loop–recombination intermediates during DNA repair (*4*). If RTEL1 acts similarly on meiotic recombination intermediates, it could be the key protein required to execute NCOs by promoting meiotic synthesis-dependent strand annealing (SDSA). By genetic measurements, recombination in *C. elegans rtel-1* mutants was significantly increased in five genetic intervals on three chromosomes, including both chromosome center and arm regions (Fig. 1A and table S1)

[1]DNA Damage Response Laboratory, London Research Institute, Cancer Research UK, Clare Hall, South Mimms, EN6 3LD, UK. [2]Howard Hughes Medical Institute, Department of Molecular and Cell Biology, University of California at Berkeley, Berkeley, CA 97420, USA. [3]Genetic Recombination Laboratory, London Research Institute, Cancer Research UK, Clare Hall, South Mimms, EN6 3LD, UK. [4]Department of Medical Genetics, Faculty of Medicine, University of British Columbia, Vancouver, BC, V6T 1Z4, Canada.

*Present address: Department of Cellular and Molecular Pharmacology, University of California, San Francisco, San Francisco, CA, 94518–2517, USA.
†To whom correspondence should be addressed. E-mail: simon.boulton@cancer.org.uk